Controlled Generation and Steering of Spatial Gap Solitons

Dragomir Neshev, Andrey A. Sukhorukov, Brendan Hanna, Wieslaw Krolikowski, and Yuri S. Kivshar

Nonlinear Physics Centre and Laser Physics Centre, Centre for Ultra-high bandwidth Devices for Optical Systems (CUDOS), Research School of Physical Sciences and Engineering, Australian National University, Canberra, ACT 0200, Australia

(Received 28 November 2003; published 19 August 2004)

We demonstrate the first fully controlled generation of *immobile and slow spatial gap solitons* in nonlinear periodic systems with band-gap spectra, and observe the key features of gap solitons that distinguish them from discrete solitons, including a dynamical transformation of gap solitons due to *nonlinear interband coupling*. We also describe theoretically and confirm experimentally the effect of the *anomalous steering* of gap solitons in optically induced photonic lattices.

DOI: 10.1103/PhysRevLett.93.083905 PACS numbers: 42.65.Tg, 42.65.Jx, 42.70.Qs

Nonlinear self-action is known to suppress wave spreading due to dispersion or diffraction and can lead to the formation of *solitary waves* (or *solitons*). Two decades ago, it was suggested that the systems with periodically modulated parameters can support a novel type of solitons—*gap solitons* [1,2]; such solitons exist in band gaps of the linear spectra in various structures including fiber Bragg gratings [3], photonic crystals [4], and Bose-Einstein condensates loaded onto optical lattices [5]. Gap solitons are composed of the forward- and backward-propagating waves which are coupled nonlinearly, and both experience Bragg scattering from the periodic structure. The strongest coupling occurs when the wave amplitudes are balanced, corresponding to the formation of *slow* or *immobile* gap solitons. In this regime, the specific dispersion [3] and stability properties [6] of gap solitons become most evident. These unique properties remain largely unexplored due to the fact that an exact balance between forward- and backward-propagating waves was not achieved, and only some reduction of the soliton velocity was observed experimentally in fiber Bragg gratings [7] and waveguide arrays [8]. This limitation is inherent due to the "side-on" excitation geometry used in the experiments, where the forward-propagating wave is launched into the periodic structure and smaller-amplitude backward wave is generated through the Bragg scattering, not allowing a direct control of the soliton velocity.

In this Letter, we study experimentally the formation of gap solitons in periodic optically induced photonic lattices where the probe laser beams experience modulation of the optical refractive index in the transverse spatial dimension, similar to waveguide arrays [9]. We implement a novel approach launching simultaneously the forward- and backward-propagating waves directly into the periodic structure. This allows us to demonstrate the first fully controlled generation of spatial gap solitons where the *soliton power and velocity can be changed independently*. In particular, we observe experimentally *immobile gap solitons*. Waveguide arrays and photonic lattices are known to support discrete solitons [9], and, in addition, this gives us an opportunity to compare both types of optical solitons emphasizing the intriguing properties of gap solitons.

In order to determine the conditions for experimental generation of spatial gap solitons and also underline their unique features in comparison with discrete solitons, we perform theoretical analysis of spatial beam propagation using the normalized paraxial equation for the electric field envelope $E(x, z)$,

$$i\frac{\partial E}{\partial z} + D\frac{\partial^2 E}{\partial x^2} + \mathcal{F}(x, |E|^2)E = 0, \tag{1}$$

where x and z are the transverse and propagation coordinates normalized to the characteristic values x_0 and z_0, respectively, $D = z_0\lambda/(4\pi n_0 x_0^2)$ is the beam diffraction coefficient, n_0 is the average medium refractive index, and λ is the vacuum wavelength. Our experiments are performed using a dynamically induced lattice in a biased photorefractive crystal [10,11], where the optically induced change of the refractive index is $\mathcal{F}(x, |E|^2) = -\gamma[I_b + I_g\cos^2(\pi x/d) + |E|^2]^{-1}$, I_b is the constant dark irradiance, I_g is the peak intensity of the two-beam interference pattern which induces the lattice with a period d, and γ is a nonlinear coefficient proportional to the applied dc field. To match our experimental conditions, we use the following parameters: $\lambda = 0.532$ μm, $n_0 = 2.4$, $x_0 = 1$ μm, $z_0 = 1$ mm, $d = 22.2$, $I_b = 1$, $I_g = 1$, $\gamma = 5.31$, and the crystal length $L = 15$ mm.

The existence of solitons is closely linked to the structure of the linear wave spectrum. In periodic lattices, the spectrum is composed of bands which correspond to the propagating *Floquet-Bloch modes* separated by gaps where the wave propagation is forbidden. The Floquet-Bloch modes are periodic solutions of linearized Eq. (1) of the form $E_{\kappa,n}(x, z) = \psi_{\kappa,n}(x)\exp(i\kappa x/d + i\beta_{\kappa,n}z)$, where $\beta_{\kappa,n}$ and κ are the Bloch-wave propagation constant and wave number, respectively, the index $n = 1, 2, \ldots$ marks the order of the transmission band, and $\psi_{\kappa,n}(x)$ has the periodicity of the lattice. In Fig. 1(a), we plot the dispersion relation $\beta_{\kappa,n}$ and mark two types of

the band gaps: the top gap, which exists due to the effect of the total internal reflection and extends to $\beta \to +\infty$, and the lower gap, which has a finite width and appears due to Bragg scattering.

Bright spatial solitons are self-trapped localized beams, which do not change during propagation due to a balance between diffraction and nonlinearity. The corresponding solutions of the model Eq. (1) have the form $E_{\kappa,n}(x, z) = u(x; \beta) \exp(i\beta z)$, where $u(x; \beta)$ is the soliton profile, and β is the propagation constant. Solitons can exist when β belongs to a spectral gap. In the case of *self-defocusing* nonlinearity ($\gamma < 0$), solitons do not exist in the total internal reflection gap. Instead, the staggered solitons may appear near the lower edge of the first band; their dispersion and steering properties resemble closely those of the discrete solitons in self-focusing media which are associated with coupling between the guided modes confined to the lattice maxima of the refractive index [10,12].

We consider the case of a *self-focusing* nonlinearity ($\gamma > 0$), where discrete and gap solitons can coexist in the same lattice and their characteristics can be compared directly; see Fig. 2. The plots are presented for the solitons centered at a maximum (on-site) and a minimum (off-site) of the lattice. At high powers, discrete solitons become localized at one or two neighboring lattice maxima, and this defines their minimum widths. In contrast, the power of gap solitons is bounded from above because the Bragg-reflection gap has a finite width, and the spectrum of the maximum soliton localization should be inside the gap [3,13]. The off-site solitons are unstable and tend to transform into their on-site counterparts; however, the instability growth rate for gap solitons is smaller than that for discrete solitons due to a bounded soliton power and width in the gap (see Fig. 2). On the other hand, gap solitons can become unstable due to interband coupling [14], whereas such instability does not exist for discrete solitons.

In periodic systems, gap solitons have the profiles closely resembling modulated Bloch waves near the corresponding band edges [14]. Therefore, controlled experimental excitation of spatial gap solitons can be realized if the modulated Bloch-wave profile is properly matched at the input. Since the Bloch waves are periodic, they can be decomposed into the Fourier series, $E_{\kappa,n}(x, 0) = \sum_m C_n(\kappa + 2\pi m) \exp[ix(\kappa + 2\pi m)/d]$. In Fig. 1(b), we show the characteristic profiles of the Bloch waves, and also plot the contribution from the leading-order Fourier components (dashed lines). In the leading order, we find $E_{0,1} = C_1(0) + \ldots$, and, therefore, lattice solitons in the semi-infinite total internal reflection gap can be generated by *a single incident beam,* as was realized in earlier experiments for arrays of weakly coupled optical waveguides [9]. On the contrary, the Bloch waves in the Bragg-reflection gap are composed of *counterpropagating waves,* e.g., $E_{\pi,n} = C_n(\pi) \exp(i\pi x/d) + C_n(-\pi) \times \exp(-i\pi x/d) + \ldots$ for $n = 1, 2$. Therefore, spatial gap solitons can be generated by using *two Gaussian beams* which are tuned to the Bragg resonance and have opposite inclination angles, as was originally suggested in Ref. [15] and further developed in Ref. [13]. Therefore, we consider the input field in the form, $E_0(x) = \sqrt{I_0} e^{-(x-x_c)^2/w^2} \cos[\pi(x - x_s)/d]$, where the exponential term approximates the gap-soliton envelope, w being

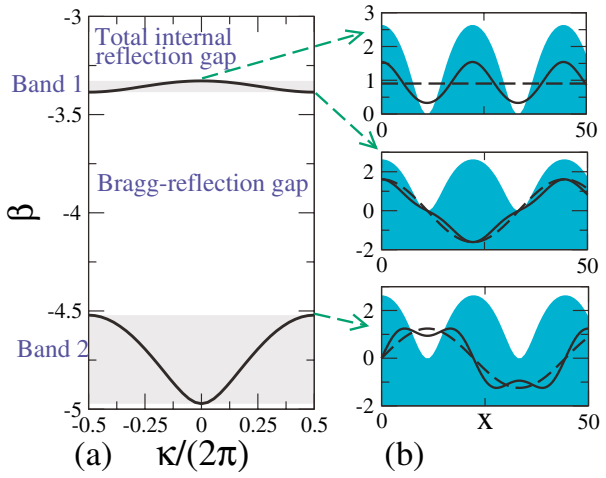

FIG. 1 (color online). (a) Dispersion of Bloch waves in an optically induced photonic lattice; the spectrum bands are shaded. (b) Profiles of the Bloch waves (solid lines) and the leading-order Fourier components (dashed lines) superimposed on top of the normalized refracted index profile of the periodic lattice (shown with shading) for gap edges indicated by arrows.

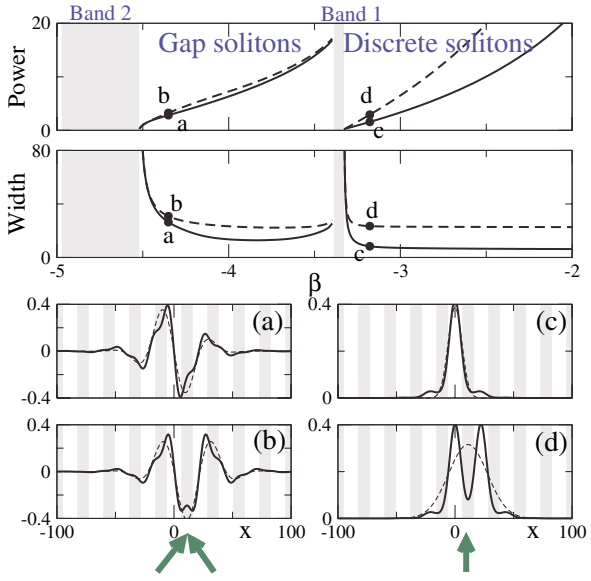

FIG. 2 (color online). Numerical results for the soliton families: Power (top) and width (middle) vs the propagation constant. Bottom: soliton profiles (solid lines) corresponding to the marked points (a–d) in the upper plots; shadings mark the lattice minima. Arrows illustrate the direction of the input beams, whose interference pattern (dashed lines) approximates the soliton profile.

the width of the input beams. The interference term approximates the Bloch-wave profile, with the shift x_s depending on the relative phase difference between the two beams. When the interference maxima are at the minima of the refractive index profile, the Bloch mode is excited at the lower edge of the Bragg-reflection gap, and the input pattern can well match the gap-soliton profile, as shown in Figs. 2(a) and 2(b).

We investigated the dynamics of the two-beam mutual focusing and the gap-soliton generation by simulating the model Eq. (1) with the input parameter x_s chosen to match the Bloch-wave profile at the lower gap edge, and $x_c = d/2$. The beams diffract at a low input power [Fig. 3(a)], whereas an immobile gap soliton forms when the input power is increased [Fig. 3(b)]. The required power depends on the input beam width, as follows from Fig. 2, and the minimum soliton width defines the fundamental limit on the degree of two-beam mutual focusing. Indeed, as the power grows, a gap-soliton breaks up through a resonant excitation of the first band, and subsequent formation of a quasiperiodic breathing mode [Fig. 3(c)]. These effects are generic, and they may occur in lattices with various geometries [13]; the breathing states were recently observed in waveguide arrays [16].

Our experiments were performed in a 15 mm long strontium barium niobate (SBN:60) crystal externally biased along the crystalline c axis. The experimental scheme is sketched in Fig. 4 (top-left panel), where two extraordinary polarized probe beams were focused by cylindrical lens and made to overlap at the input face of the crystal (see auxiliary figure in Ref. [17] for details).

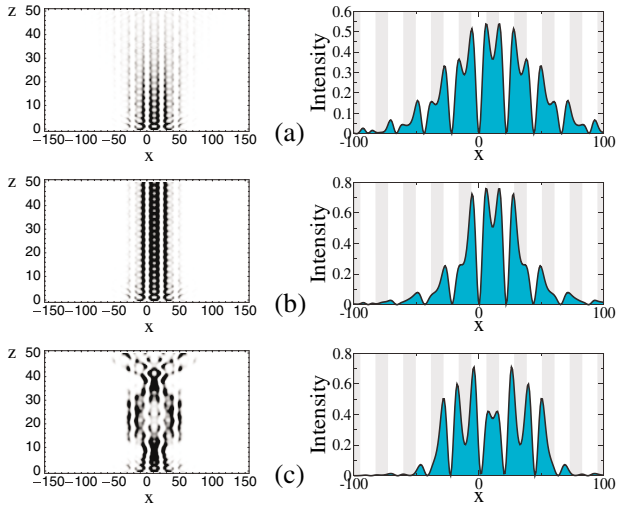

FIG. 3 (color online). Numerical results. Dynamics of the Bloch waves excited through the two-beam interference: (a) linear diffraction at low power ($I_0 \simeq 0$), (b) excitation of a gap soliton in the nonlinear regime ($I_0 = 0.048$), (c) beam breakup and the formation of a quasiperiodic breathing state at higher powers ($I_0 = 0.29$). Left: variation of intensity along the propagation direction. Right: beam profiles at the crystal output ($z = 15$ mm) normalized to I_0.

The angle between these two beams was set to twice the Bragg angle, such that the periodicity of the interference pattern is equal to that of the lattice (22 μm). In our case, the value of periodicity corresponds to a relatively wide gap in the transmission spectrum, as shown in Fig. 1(a). The relative phase between the probe beams was tuned to obtain a symmetric interference pattern corresponding to the off-site state ($x_c = d/2$), as shown in Fig. 4 (top, right). The relative position between this pattern and the lattice could also be controlled, by changing the relative phase between the two lattice-forming beams [11]. The input width of the overlapping probe beams is $w = 55$ μm (65 μm FWHM). For a zero bias field, when the lattice is absent, the beams become fully separated at the crystal output. When an electric field of 5000 V/cm is applied to the crystal, the interference pattern induces a periodic modulation of the optical refractive index and the probe beams excite Bloch waves at the edge of the Brillouin zone corresponding to the first or the second band, depending on the relative position of the lattice.

The experimental results shown in Fig. 4 confirm remarkably all theoretical predictions. First, we align the interference maxima of the input beams with the minima of the induced lattice at the input face of the crystal and record the beam profiles at the back face for several input powers [see Fig. 4 (left column)]. The output intensity is exactly zero at the maxima of the index grating. The intensity maxima are out of phase, as con-

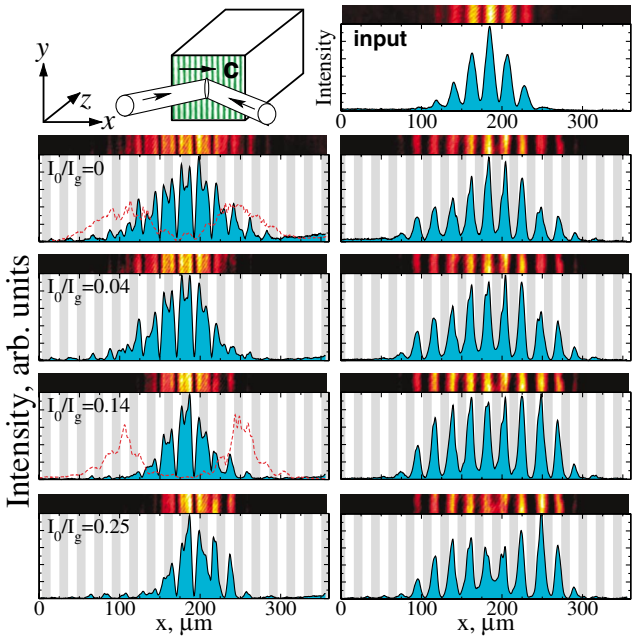

FIG. 4 (color online). Experimental results. Top: Excitation scheme (left) and input intensity profile (right). Bottom: output for various beam powers. Left: mutual focusing and gap-soliton formation when interference maxima are aligned with the lattice minima. Right: Self-defocusing when interference maxima are at the lattice maxima. Dashed curves: The beam profiles at the indicated intensity when the grating is erased.

firmed with interferometric measurements, and possess a double peak structure located at the minima of the grating. At low powers, the output intensity pattern is broad and corresponds to the Bloch waves at the lower gap edge. The beam is centered exactly between two unperturbed output beams [dashed curve in Fig. 4 (left column)] measured for zero voltage. At higher intensity ($I_0/I_g = 0.04$), we observe the two beam mutual focusing. For intensities $I_0/I_g = 0.14$, the output beam becomes self-trapped to a state which has the width equal to that at the input [see Fig. 4 (left column)], indicating the formation of a spatial gap soliton. The gap soliton has zero transverse velocity and is centered between the two output beams that separate when the grating is erased (dashed curve). As predicted theoretically, the effect of the mutual focusing is limited, and at higher intensities ($I_0/I_g = 0.25$) the beam disintegrates [see Fig. 4 (left column, bottom plot)] while its profile becomes asymmetric due to the diffusion contribution to the photorefractive nonlinearity. On the other hand, when we align the interference maxima of the input beams at the lattice maxima, the excited Bloch-wave corresponds to the upper edge of the Bragg-reflection gap (see Fig. 1) and it experience anomalous diffraction [18] leading to self-defocusing as the power is increased [Fig. 4(right)].

Finally, we study mobility of spatial gap solitons. Experimentally, the soliton steering is induced by tilting the lattice by 20% of the Bragg angle, thus introducing *a lateral shift* of the induced waveguides by 16 μm at the output [the lattice is shifted to the right in Fig. 5(a)]. Results of our experiments and the corresponding numerical simulations are presented side by side in Figs. 5(b) and 5(c); they show that the generated gap solitons *move to the left* when the grating is *tilted to the right*. In the experimental profile, a small excitation of the first band can be seen on the right-hand side (positive x) of the gap soliton. It appears due to small asymmetry of the initial excitation profile and inhomogeneities of the lattice. The *anomalous steering* is observed because the spatial group-velocity dispersion (GVD) for gap solitons of the second band is almost 3 times larger compared to a homogeneous medium under our experimental conditions. This phenomenon is analogous to *the superprism effect in photonic crystals* in the spatial domain [19]. By changing the lattice period and modulation depth, we can increase or decrease the GVD of gap solitons. In contrast, the discrete solitons associated with the first band always experience reduced spatial GVD, and therefore tend to propagate along the lattice [20].

In conclusion, we have demonstrated experimentally the first fully controlled generation of spatial gap solitons in optically induced periodic photonic lattices and observed novel effects such as anomalous steering of gap solitons and the limitation of the two-beam mutual focusing through interband coupling. We believe our results

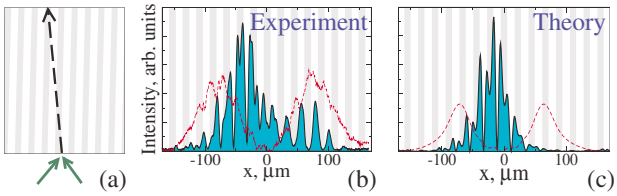

FIG. 5 (color online). (a) Schematic demonstration of anomalous gap-soliton steering induced by a tilt of the lattice; dashed line shows the propagation direction of a gap soliton; arrows indicate the directions of the input beams. (b),(c) Output soliton profile for a lattice tilt in the direction of larger x by 20% of the Bragg angle with respect to normal; dashed lines show the beam profiles when the lattice is absent.

can also be useful for the study of nonlinear effects in photonic crystals and nonlinear dynamics of the Bose-Einstein condensates in optical lattices.

Note added.—Independent observation of immobile spatial gap solitons was recently reported in Ref. [21].

[1] Yu. I. Voloshchenko *et al.*, Zh. Tekh. Fiz. **51**, 902 (1981) (in Russian) [Sov. Phys. Tech. Phys. **26**, 541 (1981)].
[2] W. Chen and D. L. Mills, Phys. Rev. Lett. **58**, 160 (1987).
[3] C. M. de Sterke and J. E. Sipe, in *Progress in Optics*, edited by E. Wolf (North-Holland, Amsterdam, 1994), Vol. XXXIII, pp. 203–260.
[4] N. Akozbek and S. John, Phys. Rev. E **57**, 2287 (1998).
[5] O. Zobay *et al.*, Phys. Rev. A **59**, 643 (1999).
[6] I.V. Barashenkov *et al.*, Phys. Rev. Lett. **80**, 5117 (1998).
[7] B. J. Eggleton *et al.*, Phys. Rev. Lett. **76**, 1627 (1996).
[8] D. Mandelik *et al.*, Phys. Rev. Lett. **90**, 053902 (2003).
[9] D. N. Christodoulides *et al.*, Nature (London) **424**, 817 (2003).
[10] J.W. Fleischer *et al.*, Phys. Rev. Lett. **90**, 023902 (2003).
[11] D. Neshev *et al.*, Opt. Lett. **28**, 710 (2003).
[12] Yu. S. Kivshar, Opt. Lett. **18**, 1147 (1993).
[13] A. A. Sukhorukov and Yu. S. Kivshar, Opt. Lett. **28**, 2345 (2003).
[14] D. E. Pelinovsky *et al.*, nlin-PS/0405019.
[15] J. Feng, Opt. Lett. **18**, 1302 (1993).
[16] D. Mandelik *et al.*, Phys. Rev. Lett. **90**, 253902 (2003).
[17] See EPAPS Document No. E-PRLTAO-93-048433 for the experimental setup scheme. A direct link to this document may be found in the online article's HTML reference section. The document may also be reached via the EPAPS homepage (http://www.aip.org/pubservs/epaps.html) or from ftp.aip.org in the directory /epaps/. See the EPAPS homepage for more information.
[18] R. Morandotti *et al.*, Phys. Rev. Lett. **86**, 3296 (2001).
[19] P. St. J. Russell *et al.*, in *Confined Electrons and Photons: New Physics and Applications*, edited by E. Burstein and C. Weisbuch (Plenum Press, New York, 1995), pp. 585–633.
[20] R. Morandotti *et al.*, Phys. Rev. Lett. **83**, 2726 (1999).
[21] D. Mandelik *et al.*, Phys. Rev. Lett. **92**, 093904 (2004).